

## MODELING OF FISCHER–TROPSCH SYNTHESIS PACKED BED REACTOR FOR PRODUCING LIQUID FUELS FROM NATURAL GAS

Mohammad Irani

Gas Division, Research Institute of Petroleum Industry (RIPI), Tehran, Iran.

Received January 2, 2013, Accepted March 30, 2013

---

### Abstract

A tubular pilot scale fixed-bed reactor for the Fischer–Tropsch Synthesis (FTS) was simulated to numerically demonstrate the conversion of synthesis gas ( $\text{CO}+\text{H}_2$ ) to higher hydrocarbons over an iron based catalyst. The reactor was a 3.1 cm diameter and 2.75 m length steel tube. The feed temperature were between 563- 583 K. Saturated water was employed to control the peak temperature within the catalyst bed, which is critical for the stability of iron based catalyst. In this research, computational fluid dynamics (CFD) was used to model the interacting phenomena such as non-ideality of mixture, reaction and hydrodynamics in a fixed-bed reactor for the FTS. Synthesis gas conversion, product selectivity, and temperature were measured as a function of reactor length. FTS can be conducted with very low temperature range between 563 and 583K within a wide range of CO conversion using saturated water as coolant. By using saturated water, reactor exhibited good isothermal condition under most simulated conditions. Very good agreement between pilot experimental data and the model was achieved. Results show that increase in feed temperature have a significant effect on the yield of products.

**Keywords:** Numerical modeling; Fischer–Tropsch synthesis; packed reactor; CFD methods; saturated water.

---

### 1.Introduction

The Fischer–Tropsch synthesis (FTS) is a key step in the conversion of natural gas and coal or biomass into liquid fuels (synfuels) through the so-called gas-to-liquids (GTL) and coal/biomass-to-liquids (CTL/BTL) processes. Among them, GTL is particularly attractive from the point of view of operating costs, carbon and thermal efficiencies as well as environmental impact [1-3]. The FTS is the catalytic conversion of synthesis gas ( $\text{CO}+\text{H}_2$ ) into a multi-component mixture of hydrocarbons and water. The commercial FTS plants have utilized either Fe or Co catalysts using FTS to produce liquid fuels (gasoline and diesel) [4, 5]. The FTS can be viewed as a polymerization reaction where chain growth is the basic feature. Various types of reactors (including fluidized bed, multi-tubular fixed-bed and slurry) have been considered during the FTS process development. The fixed-bed FT process, being one of the most competing reactor technologies, occupies a special position in FTS industrial processes [6-9]. Due to the high demand on gasoline in the world and its higher price relative to that of diesel, production of gasoline from the FT process, becomes more favorable. The octane number of FT gasoline is lower than that of the gasoline obtained from crude oil processing, since the FT gasoline mainly consists of n-paraffin. To promote the yield and quality of the gasoline from FTS, bi-functional catalysts have received extensive attention in the recent years [10].

In this research, the modified bi-functional Fe-HZSM5 catalyst has been used. Such a process removes the need for cumbersome upgrading units for GTL plants [11]. To achieve optimum condition for the best performance of process, the reactor should be simulated exactly by considering non-idealities. Clearly, due to the complexity of FTS reaction system, variety of products ( $\text{C}_1\text{-C}_{20}$ ) and operating condition of this process, a suitable reactor model with considering thermodynamic non-idealities, from which the selectivity and heat transfer information can be determined in a qualitative fashion, has not been presented yet [12,13].

Bub *et al.* [14] and Jess *et al.* [15] developed a two-dimensional, pseudo-homogeneous model that was used to predict product distribution and performed the conceptual design of a fixed-bed

reactor for converting nitrogen rich syngas. Atwood and Bennet [16] have proposed a one-dimensional, homogeneous plug flow model. Wang *et al.* [17] devised a comprehensive one-dimensional heterogeneous reactor model to simulate the performance of fixed-bed FT reactors for hydrocarbon production. Liu *et al.* [18] have studied the steady state and dynamic behavior of the FT fixed-bed reactor using a two-dimensional heterogeneous model. Also, Marvast *et al.* [19] have simulated the behavior of the FT fixed-bed reactor using a two-dimensional heterogeneous model at steady state condition.

In the present work, we report a computational fluid dynamic (CFD) study to investigate performance of a bi-functional Fe-HZSM-5 catalyst in a pilot scale tubular fixed-bed reactor for FTS, coupling the exothermic FTS with saturated water for heat removal. The CFD is a powerful tool for simulating complex reacting flows [20-24]. The aim of our study was to analyze the conditions under which the synthesis reaction could be conducted at a reasonably high CO conversion close to the isothermal condition at temperatures between 563 and 583 K. The simulation results have been validated with pilot experimental data.

## 2. Process description

The FTS has been investigated in a pilot scale of a fixed bed reactor which was packed with bi-functional Fe-HZSM5 catalyst (metal part: 100 Fe/5.4 Cu/7K2O/21SiO2, acidic part: SiO2/Al2O3=14). There was a jacket around the reactor which boiling water flowing through it to remove the heat of reaction. The temperature of boiling water could be controlled measuring pressure of the system. The pilot has been designed and constructed by the Research Institute of Petroleum Industry, National Iranian Oil Company (RIPI-NIOC) in 2008 [12]. The characteristics of the pilot plant are shown in Table 1. The object is to find the profiles of temperature and concentration of various species along the fixed-bed reactor length at different conditions and recognize the optimum condition.

Table1 FTS pilot plant characteristics

Tube Dimension(mm)	31×3×2.75
Number of tubes	1
Molar Ratio of H2/Co	1
Feed Temperature(K)	563,573 and 583
Catalyst sizes (mm)	1.5×4
Catalyst density(kg/m <sup>3</sup> )	1290
Bulk density(kg/m <sup>3</sup> )	730
Reactor pressure(bar)	17
Cooling temperature (K)	Saturated water (563,573 and 583)
GHSV(Nl/hr)	3
Bed Voidage	0.38

## 3. Mathematical Model

### 3.1. Governing equations

In order to model the problem, five sets of equations should be solved; continuity equation, momentum balance, energy and species transport equations. The mass conservation, momentum, and total enthalpy equations, may be expressed as follows, respectively:

$$\nabla \cdot (\vec{v} \rho) = 0 \quad (1)$$

$$\nabla \cdot (\rho \vec{v} \vec{v}) = -\nabla P + \nabla \cdot [\mu (\nabla \vec{v} + \nabla \vec{v}^T)] + \rho g + S \quad (2)$$

$$\nabla \cdot (\vec{v} (\rho H + P)) + \nabla \cdot \left( \sum_{i=1}^n h_i j_i \right) = -\nabla \cdot (q) + S_R \quad (3)$$

$$\nabla \cdot (\vec{v} C_i - D_i \nabla C_i) = R_i \quad (4)$$

$$S = - \left( \sum_{j=1}^2 D_{ij} \mu v_j + \sum_{j=1}^2 C_{ij} \frac{1}{2} \rho |v| v_j \right) \quad S_R = - \left( \sum_j \frac{h_j^0}{M_j} R_j \right) \quad (5)$$

Where,  $\rho$  represents mixture density,  $\vec{v}$  is velocity vector, and  $H$ ,  $h_i$  are total enthalpy and enthalpy of species, respectively and  $C_i$  stands for concentration of chemical species.  $P$  is the static pressure,  $S$  is the model-dependent source term from porous-media and  $S_R$  is the heat of reaction. The catalyst zone considered as a porous media that modeled by the addition of a momentum source term to the standard momentum equation. The source term is composed of two parts: a viscous loss term (Darcy, the first term on the right-hand side of Equation 5) and an inertial loss term (the second term on the right-hand side of Equation 5).  $|v|$  is the magnitude of the velocity and  $D$  and  $C$  are prescribed matrices. The momentum sink contributes to the pressure gradient in the porous cells, causing a pressure drop that is proportional to the fluid velocity in the cells [25].

Due to complexity of the FTS reaction system, variety of products ( $C_1$ -  $C_{20}$ ) and operating condition of the process, non-ideal thermodynamic behavior of system should be considered using Eqs 6 to 8 [12,13]. Hereupon, a suitable EOS (equation of state) should be used for calculation of mixture density and species fugacity ( $f_i$ ). For this study Peng-Rabinson equation was chosen as a suitable EOS which its parameters has been listed in table 2.

Table 2 Parameters of Peng-Rabinson EOS

$\sigma$	$\varepsilon$	$\Omega$	$\Psi$
$1 + \sqrt{2}$	$1 - \sqrt{2}$	0.07779	0.45724

$$\alpha(T_r; \omega) = \left[ 1 + (0.37464 + 1.54226\omega - 0.26992\omega^2) \left( 1 - T_r^{1/2} \right) \right]^2$$

$$Z = \beta + (Z + \varepsilon\beta)(Z + \sigma\beta) \left( \frac{1 + \beta - Z}{q\beta} \right) \quad , \beta = \Omega \frac{P_r}{T_r} \quad , \quad q = \frac{\alpha(T_r)\Psi}{\Omega T_r}$$

$$\ln \hat{\varphi}_i = (Z - 1) \frac{b_i}{b_m} - \ln(Z - \beta) - I \bar{q}_i$$

$$q = \frac{a}{bRT}$$

$$\bar{q}_i = q \left( 2 \times \frac{\frac{\partial a}{\partial x_i}}{a} - \frac{b_i[i]}{b} \right) \quad (6)$$

$$I = \frac{1}{\varepsilon_1 - \varepsilon_2} \ln \left( \frac{Z + \varepsilon_1 \times \beta}{Z + \varepsilon_2 \times \beta} \right)$$

$$\beta = \frac{bP}{RT}$$

$$f_i = \hat{\varphi}_i \times P \times y_i$$

### 3.2 Computational domain and boundary conditions

The schematic of the setup is given in figure1, A two- dimensional system (2.75 m x 31mm) which was fed with synthesis gas (a mixture of carbon monoxide and hydrogen). Furthermore, the reactor was divided in two sections: 1) top zone fluid, 2) reaction (catalyst) zone. Packed

bed was considered as a porous media due to the large value of  $N$  (tube-to-catalyst diameter ratio) [26].

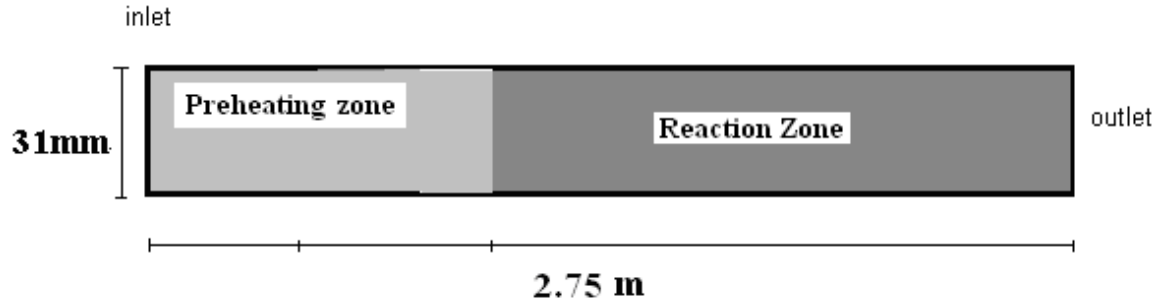


Figure.1 Schematic of fixed-bed reactor and its boundary conditions

The mass-flow-inlet boundary condition was used for gas flow to the modeled reactor. The pressure-outlet boundary condition was specified at the bottom of the reactor. The FTS reaction is exothermic and if the heat of reaction isn't removed, temperature run away will be taken place. In this study saturated water was used for heat removal, so heat absorbed by water generates steam and reactor was assumed to be isothermal. The source term ( $S$ ) for boundary cells (walls in reaction zone) should be included as follows:

$$S = -(H(T') - H(T)) \quad (7)$$

Which  $H(T')$  is enthalpy at temperature  $T'$  (the increased temperature due to releasing heat of reaction) and  $H(T)$  is enthalpy at temperature  $T$  (the desired temperature for reaction).

### 3.3. Products and rate equations

When rate equations include in the CFD simulation, chemical kinetic calculations are very computer time consuming, especially for a complex reaction scheme like FTS [17]. In some simulation studies the complexity of the FTS chemistry has been reduced by using a set of global one-step reaction for selected mechanism [19]. The Fischer-Tropsch reactants and products which considered in this study consist of:  $CO$ ,  $H_2$ ,  $CO$ ,  $CO_2$ ,  $H_2O$ ,  $CH_4$ ,  $C_2H_4$ ,  $C_2H_6$ ,  $C_3H_8$ ,  $n-C_4H_{10}$ ,  $i-C_4H_{10}$  and  $C_5+$ . The following reactions listed in Table 3 are leading Fischer-Tropsch reactions [27]:

Table 3 List of FTS reactions

Num.	Reaction stoichiometry
1	$CO + 3H_2 \longrightarrow CH_4 + H_2O$
2	$2CO + 4H_2 \longrightarrow C_2H_4 + 2H_2O$
3	$2CO + 5H_2 \longrightarrow C_2H_6 + 2H_2O$
4	$3CO + 7H_2 \longrightarrow C_3H_8 + 3H_2O$
5	$4CO + 9H_2 \longrightarrow n-C_4H_{10} + 4H_2O$
6	$4CO + 9H_2 \longrightarrow i-C_4H_{10} + 4H_2O$
7	$8.96CO + 18.05H_2 \longrightarrow C_{8.96}H_{12.36}(C_5^+) + 8.96H_2O$
8	$CO + H_2O \longrightarrow CO_2 + H_2$

The general form of reaction rate equation is like Eq. (8) and for FTS its kinetic parameters [27] are given in table 4:

$$R_i \left( \frac{mol}{hr.gr_{cat}} \right) = k_i \exp \left( \frac{-E_i}{RT} \right) \frac{f_{h_2}^2}{f_{co}} \quad (8)$$

Table 4 FTS parameters of reaction rates

	$K_1(\text{mol s}^{-1} \text{ kg}_{\text{cat}}^{-1}/\text{kPa})$	$E_i(\text{J mol}^{-1})$
1	2.044 e-2	15693
2	6.255 e-5	20.384
3	3.423 e-4	1.5607
4	5.972 e-6	164.06
5	6.482 e-6	86.934
6	6.482 e-6	81.753
7	3.168 e-5	738.78
8	3.168 e-5	5532.9

### 3.4. Material properties

The specific heat of each species was defined as piecewise-polynomial function of temperature. Besides to consider variation of density with temperature and composition, compressibility factor (Z) was calculated using Peng-Rabinson EOS and also the density of gas mixture was defined as follow:

$$\rho = \frac{P \times M}{Z RT} \quad (9)$$

Where R is the universal gas constant,  $M_G$  is the molecular weight of gas mixture and P is the operating pressure (taken to be 17 bar). For other thermal properties of the mixture such as molecular viscosity, thermal conductivity and diffusivity coefficient, the relations in appendix were used [28].

The steps implemented in the solution procedure are as follows:

1. Calculation of the gas-phase transport properties.
2. Calculation of the density of gas mixture using Peng-Rabinson EOS.
3. Calculation of the thermodynamic properties such as fugacity coefficients and compressibility factors using special subroutines.
4. Determination of the rate of consumption of reactants and production of products per unit volume.
5. Determination of the source terms for all the conservation equations.
6. Solving the conservation equations.

The finite volume method has been used to discrete the partial differential equations of the model, using the SIMPLE method for pressure-velocity coupling.

## 4. RESULTS AND DISCUSSION

The geometry and grid was created in Gambit (Figure 2), the pre-processor of Fluent. The geometry consists of a rectangle, 2.75m in length and 31mm in width, with uniform structured grids to simulate fluid flow. A parametric study was done by varying the gas inlet temperature. In all cases, reactor pressure and  $\text{H}_2/\text{CO}$  ratio are kept constant at 17 bar and 1, respectively. Based on the variation of gas inlet temperatures, three set of simulations were performed.

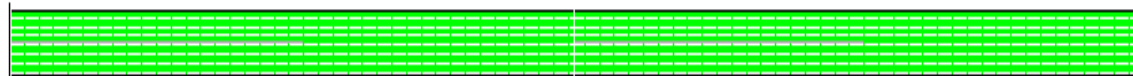


Figure 2 Mesh configuration of computational domain

Figure 3 presents the contour of velocity in the reactor. As can be seen, in the first zone of the reactor the velocity has the maximum value and in catalyst region, it is decreased due to the pressure drop in the reaction zone.

Figure 4 shows the mass fraction profiles of product species along the reactor length for the case with the inlet gas temperature of 573 K. As shown in figure 4 the mass fraction of product species is continuously increasing from the inlet to the outlet and there is a jump in

the end zone of the reactor due to the decrease in mass fraction of CO. (considering reaction rates, denominator is fugacity of CO).

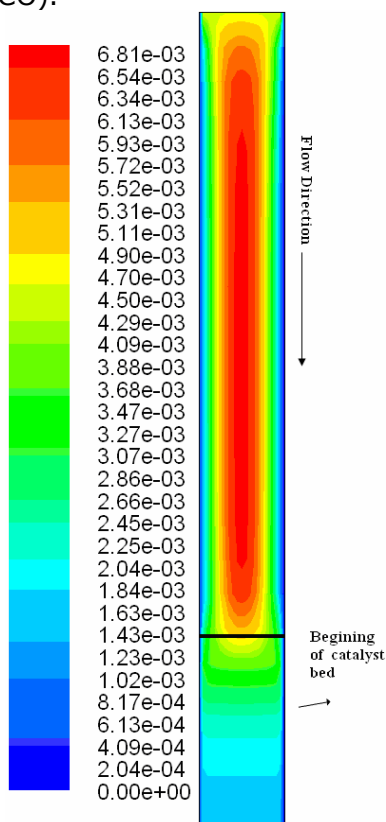


Figure.3 Contour of velocity (operating condition: T=573, P=17 bar)

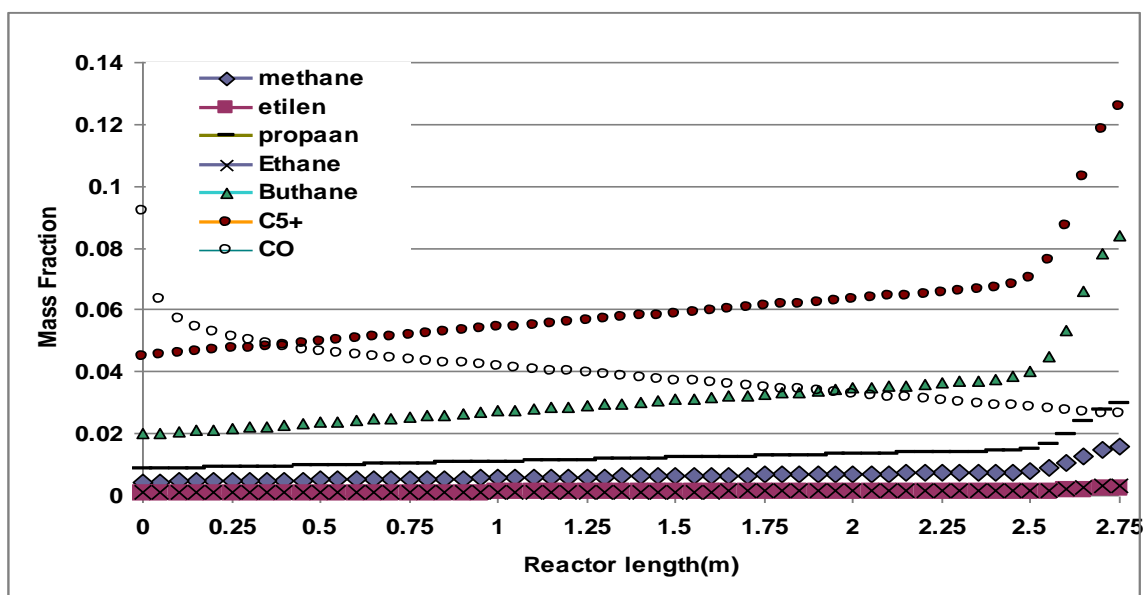


Figure. 4. Mass fraction of species along the reactor length at T=573

As depicted in figure 5 in the case with temperature of 563 the  $C_{5+}$  selectivity was less than the case with temperature of 573. When the temperature was increased to 583K,  $C_{5+}$  selectivity was declined because of activation of water-gas-shift reaction at this temperature and increasing of  $CO_2$  production.

Based on the production of heavier products in reaction zone, density increases along the reactor length (Figure 7).

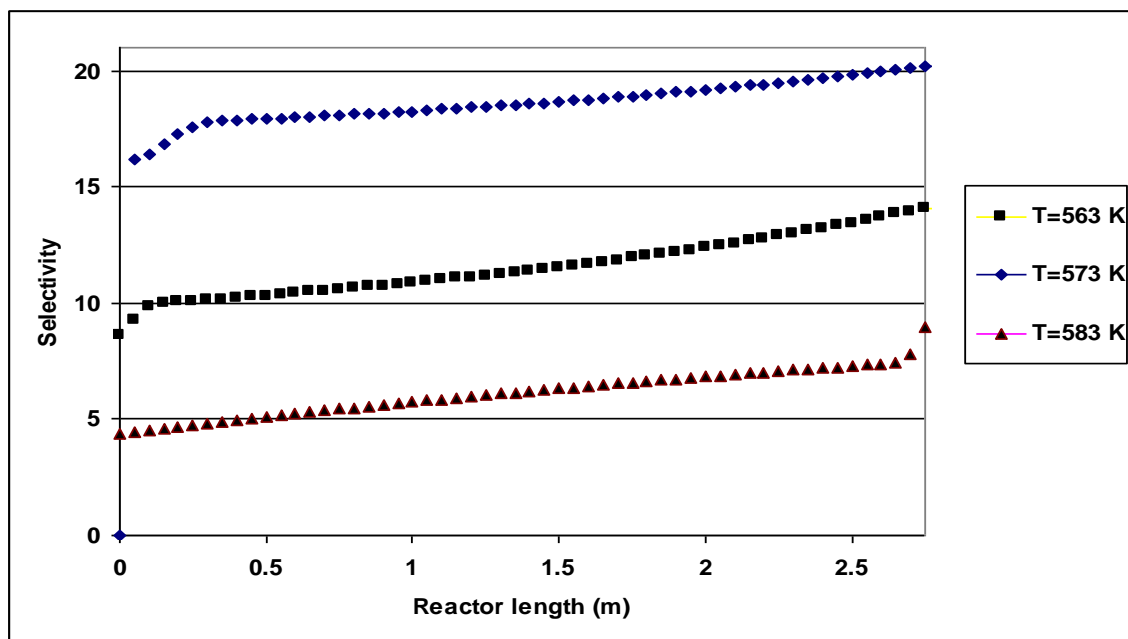


Figure. 5. Selectivity of species at different temperatures along the reactor length

#### 4.1. Control of the FTS temperature

As mentioned before, the aim of this study was to analyze the conditions that the FTS could be conducted in a fixed-bed reactor at a reasonably high CO conversion near isothermal condition at any desired reaction temperature between 563 and 583 K. To this end, a series of CFD simulations have been carried out in which the significant result of this simulation study has been confirmation of the isothermicity exhibition of the fixed-bed reactor. As an example, figure 6 shows the distribution of temperatures along the reactor length at steady state condition for a simulation conducted under conditions of T=573 K, P=17 bar.

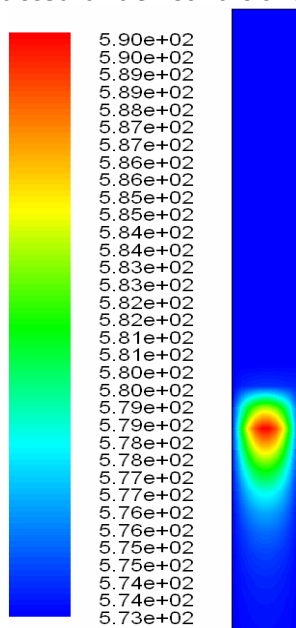


Figure.6 Contour of temperature (operating condition: T=573, P=17 bar)

As shown in this figure, temperature profiles of two cases were presented. In case 1 heat removal was done with saturated water and in case 2 without heat removal. As can be seen, the maximum difference of temperature inside the fixed-bed reactor is lower than 14K, and the mean temperature of the solid is about 575 K, close to the coolant. Interestingly, the tempe-

perature of the fluid inside the catalyst zone, where the reaction takes place, is almost constant at about 577 K, that is well-suited. If there isn't any heat removal in reactor, the temperature at the front of catalytic bed is increased to 685 K and the average temperature of the fluid in catalytic bed will remain on 650 K. This temperature is not suitable for catalyst performance and catalyst degradation will occurred. These results presage a very efficient heat exchange performance of the saturated water. It should be noted that the saturated water temperature can be controlled with pressure. The maximum change in temperature of the FTS stream inside the reactor from the entry to the exit is about 10–15 K (Figure 7). Therefore, almost isothermal FTS can be achieved by setting the operating pressure at a value which the saturation temperature of liquid water is slightly below the temperature of the FT synthesis. The pressure of boiling water system has to be reduced when the CO conversion increases, to have efficient heat-removal capacity.

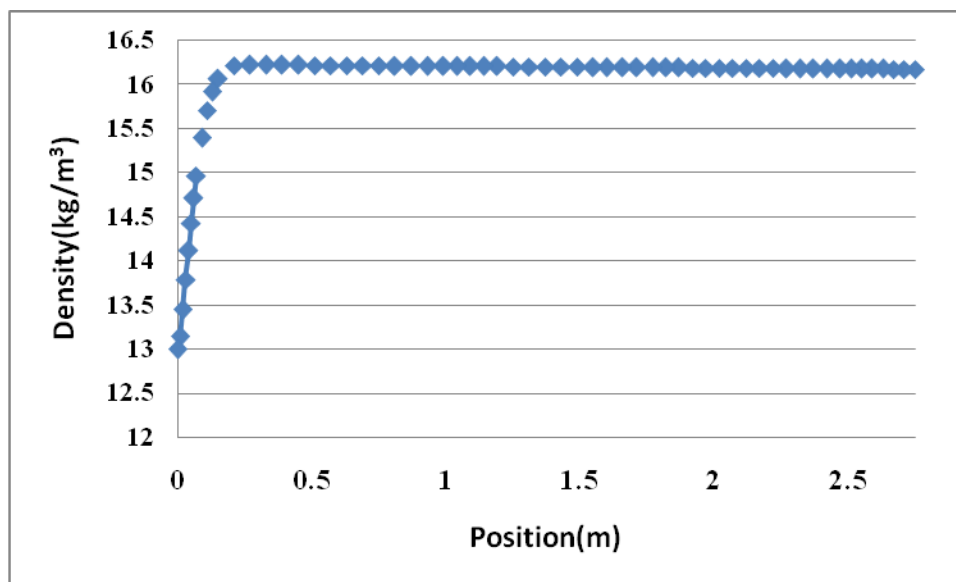


Figure.7 Profile of density (operating condition: T=573, P=17 bar)

#### 4.2. Quantitative validation

Despite the fact that the results shown in figures 3 to 8 were used for qualitative validation of the model and the solution procedure, in order to ensure the accuracy of the model, quantitative comparison of experimental data obtained from pilot and their corresponding simulated results is shown in table 5. Since it was limited to use the finite number of thermocouples, (point 1: beginning of catalytic bed; point 2: middle of catalytic bed; point 3: end of catalytic bed) only three experimental data of temperatures have been obtained and compared against their corresponding simulated results. As this table shows, the errors at all times are less than five percent, since simulation is based on the CFD approach and no empirical correlation has been used in the simulation.

Table 5 Comparison between measured and predicted values for the pilot-scale FTS processes

	experimental	simulation	Error (%)
$X_{CO}$ (%)	60.7	58.59	3.476112
C5+ selectivity (g/g feed)	18	17.29	3.944444
Temperature at point 1(K)	588	590	0.340140
Temperature at point 2(K)	575	573	0.347826
Temperature at point 3(K)	573	573	0

#### 5. Conclusions

The detailed kinetics is embedded into the reactor model. The non-ideal thermodynamic behavior of mixture is correlated by using Peng-Rabinson EOS. The reactor model is tested

against the measured data from pilot-scale and satisfactory agreements are found between predictions of model and experimental results. The numerical investigation reveals that the proposed model can allow us to gain a quantitative insight into the complicated fixed-bed FTS system. From the simulation data presented in this paper, a reactor optimization strategy can be deduced; operating at the highest possible conversion to achieve the maximum  $C_{5+}$  yield while minimizing temperature run away. The simulated reactor exhibited good isothermicity under most simulated conditions by using saturated water as heat removing system.

Increasing of feed temperature can increase syngas conversion; however it suppresses remarkably the overall yield of  $C_{5+}$  products. Therefore the selection of feed temperature is important on the premier of keeping a satisfied syngas conversion for enhancement of the overall yield of  $C_{5+}$  products.

### Nomenclature

P	Pressure, bar	T	Temperature, K
g	gravity acceleration, $m.s^{-2}$	f	fugacity, bar
v	velocity, $m.s^{-1}$	$k_i$	Kinetic Constant, $mol.hr^{-1}.gr^{-1}.bar^{-1}$
H	Total enthalpy, $kJ.kg^{-1}.s^{-1}$	$E_i$	Activation Energy, $kJ.kmol^{-1}$
h	Enthalpy of species, $kJ.kg^{-1}.s^{-1}$	R	Global Gas Factor, $kJ.kmol^{-1}.K^{-1}$
j	Mass flux, $kg.m^{-2}.s^{-1}$	$M_i$	Molecular Weight, $kg.kmol^{-1}$
q	Heat flux, $kJ.m^{-2}.s^{-1}$	V	Volume, $m^3$
S	Momentum source term,	$x_i$	mass fraction
$D_{ij}$	Diffusivity coefficient,	D	Total Diffusivity Coefficient, $m^2.s^{-1}$
$C_i$	Concentration, $kmol.m^3$	$k_m$	Thermal Conductivity, $kJ.m^{-1}.K^{-1}$
Z	Compressibility Factor		

### Greek Letters

$\rho$	Density, $kg.m^{-3}$
$\mu$	Viscosity, $kg.m^{-1}.s^{-1}$
$\varphi_i$	Fugacity coefficient

### Subscript

i	species number
j	second species number
m	mixture

### References

- [1] Bartholomew, C.H., Farrauto, R. J.: Fundamentals of Industrial Catalytic Processes, New Jersey: John Wiley & Sons Inc. – AIChE, Hoboken, 2006, 398.
- [2] Dry, M.E., Steynberg, P.: Studies in Surface Science and Catalysis, 2004, 152:406.
- [3] Davis, B.H.: Fischer–Tropsch Synthesis: Comparison of Performances of Iron and Cobalt Catalysts, *Ind. Eng. Chem. Res.*, 2007, 46 (26), pp 8938–8945.
- [4] Reidel, T., Schulz, H., Schaub, G., Jun, K., Hwang, J., Lee, K.: Topics in Catalysis, 2003, 26:41.
- [5] De Deugd, R.M., Kapteijn, F., Moulijn, J. A.: Topics in Catalysis, 2003, 26:29.
- [6] Steynberg, A.P., Dry, M. E., Havis, B.H., Berman, B. B.: Studies in Surface Science and Catalysis, 2004, 152:64.
- [7] Dry, M.E.: Practical and Theoretical Aspects of the Catalytic Fischer-Tropsch Process, Applied Catalysis A: General, 1996, 138:319.
- [8] Sie, S.T. : Process development and scale up: IV Case history of the development of a Fischer-Tropsch synthesis process, *Rev. Chem. Eng.* 1998, 14, 109–157.
- [9] Davis, B.H.: Topics in Catalysis, 2005, 32:143.
- [10] Nakhaei Pour, Zamani, Y., Tavasoli, A., Shahri, S.M. K., Taheri, S.A.: Study on products distribution of iron and iron–zeolite catalysts in Fischer–Tropsch synthesis, *Fuel*, 2008, 87:2004.
- [11] Fischer–Tropsch pilot plant of Research Institute of Petroleum Industry and National Iranian Oil Company (RIPI-NIOC), Tehran 18745-4163, Iran, 2004.
- [12] Irani, M., Bozorgmehry, R.B., Pishvaie, M. R., Tavasoli, A.: Investigating the effects of mass transfer and mixture non-ideality on multiphase flow hydrodynamics using CFD methods, *Iran. J. Chem. and Chem. Eng.*, 2009.

- [13] Irani, M., Bozorgmehry, R.B., Pishvaie, M. R.,: Impact of Thermodynamic Non-idealities and Mass Transfer on Multi-phase Hydrodynamics, *Sci. Iranica*, 2010.
- [14] Bub, G., Bearns, M., Bussemier, B., Frohning, C.: *Chemical Engineering Science*, 2003, 58:867.
- [15] Jess, A., Popp, R., Hedden, K.: Fischer-Tropsch synthesis with nitrogen-rich syngas: Fundamentals and reactor design aspects, *Applied Catalysis A*, 1999, 186:321.
- [16] Atwood, H.E., Bennet, C.O.: *Ind. Eng. Chem. Proc. Des. Dev.* 1979, 18:163.
- [17] Wang, Y.N., Xu, Y.Y., Li, Y.W., Zhao, Y.L., Zhang, B.J.: *Chem. Eng. Sci.*, 2003, 58:867.
- [18] Liu, Q. S., Zhang, Z.X., Zhou, J. L.: *J.Nat.Gas Chem.* 1999, 8:137.
- [19] Marvast, M.A., Sohrabi, M., Zarrinpashneh, S., Baghmisheh, Gh.: *Chem. Eng. and Tech.*, 2005, 1:28.
- [20] Amirshaghghi, H., Zamaniyan, A., Ebrahimi, H., Zarkesh, M.: Numerical simulation of methane partial oxidation in the burner and combustion chamber of autothermal reformer, *Applied Mathematical Modelling*, 34(2010) 2312-2322.
- [21] Jazbec, M., Fletcher, D. F., Haynes, B. S.: Simulation of the ignition of lean methane mixtures using CFD modelling and a reduced chemistry mechanism, *Applied Mathematical Modeling*, 24, 8-9(2000) 689-696.
- [22] Pougatch, K., Salcudean, Gartshore, M. I.: A numerical model of the reacting multiphase flow in a pulp digester, *Applied Mathematical Modeling*, 30 (2006) 209-230.
- [23] Shang, Z.: CFD of turbulent transport of particles behind a backward-facing step using a new model—k-e-Sp, *Applied Mathematical Modeling*, 29 (2005) 885-901.
- [24] Gerber, A.G., Dubay, R., Healy, A.: CFD-based predictive control of melt temperature in plastic injection molding, *Applied Mathematical Modeling* 30 (2006) 884-903.
- [25] Fluent, Incorporated: *FLUENT 6 USER Manual*, Lebanon (NH): Fluent Inc., 2001.
- [26] Foumeni, E.A., Moallemi, H.A., Mcgreavy, C., Castro, A.A.: *Canad. J. Chem. Eng.*, 1991, 69:1010.
- [27] Marvast, M.A.: Ph.D. Thesis, Amirkabir University of Technology: Tehran- Iran, 2005.
- [28] Poling, B.E., Prausnitz, J. M., O'Connell, J.P.: *The Properties of Gases & Liquids*, 5<sup>th</sup> ed., New York: McGraw-Hill, 2000.
- [29] Mason, E.A., Saxena, S.C.: *Phys. Fluids*, (1958) 1:361.

*Corresponding author, PhD of Chemical Engineering. postal address: Gas Division, Research Institute of Petroleum Industry (RIPI), West Blvd., Near Azadi Sports Complex, Tehran, Iran. Phone: +98 (21) 48252403, Fax: +98 (21) 44739716, E-mail address: Iranim@ripi.ir or Mohammadirani@yahoo.com*

## Appendix

Thermophysical properties in the gas phase were calculated using the following relations [28].

### Binary Diffusivity

Fuller's method was used to determine diffusivity:

$$D = 0.04357 T^{1.75} \frac{\sqrt{(M_1 + M_2)/M_1 M_2}}{P(V_1^{1/3} + V_2^{1/3})^2} \quad (\text{A.1})$$

And

$$D^{i,m} = \frac{(1-x_i)}{\sum_{j=1}^n x_j / D_{ij}} \quad (\text{A.2})$$

Where  $V_i$  is found for each component by summing atomic diffusion volumes given in [28].

### Gas-Phase Mixture Viscosity

Wilke's method has been used to determine the gas-phase viscosity. It is expressed as

$$\mu_m = \sum_{i=1}^n \frac{x_i \mu}{\sum_{j=1}^n x_j \phi_{ij}} \quad (\text{A.3})$$

Where

$$\phi_{ij} = \frac{\left[ 1 + \left( \frac{\mu_i}{\mu_j} \right)^{0.5} \left( \frac{M_j}{M_i} \right)^{0.25} \right]^2}{\left[ 8 \left( 1 + \frac{M_i}{M_j} \right) \right]^{0.5}} \quad (\text{A.4})$$

And

$$\phi_{ji} = \frac{\mu_j}{\mu_i} \frac{M_i}{M_j} \phi_{ij} \quad (\text{A.5})$$

### Gas-Phase Mixture Thermal Conductivity

Thermal conductivity of the gas mixture was determined as follows. However, an additional factor proposed by Mason and Saxena [\[29\]](#) was used:

$$k_m = \sum_{i=1}^n \frac{x_i k_i}{\sum_{j=1}^n x_j A_{ij}} \quad (\text{A.6})$$

Where

$$A_{ij} = \frac{\varepsilon \left[ 1 + \left( \frac{k_i}{k_j} \right)^{0.5} \left( \frac{M_j}{M_i} \right)^{0.25} \right]^2}{\left[ 8 \left( 1 + \frac{M_i}{M_j} \right) \right]^{0.5}} \quad (\text{A.7})$$

$$\varepsilon = 1.065$$

And

$$A_{ji} = \frac{\mu_j}{\mu_i} \frac{M_i}{M_j} A_{ij} \quad (\text{A.8})$$

### Specific heat

$$C_P^m = \sum_{i=1}^n x_i C_P^i \quad (\text{A.9})$$